Single-Point Calibration for Microwave Sounders: Application to TEMPEST-D

SHANNON T. BROWN,[a] ALAN TANNER,[a] STEVEN C. REISING,[b] AND WESLEY BERG[b]

[a] Jet Propulsion Laboratory, California Institute of Technology, Pasadena, California
[b] Colorado State University, Fort Collins, Colorado

(Manuscript received 10 June 2022, in final form 25 February 2023, accepted 2 March 2023)

ABSTRACT: Passive microwave sounders are critical for accurate forecasts from numerical weather prediction models. These sensors are calibrated using a traditional two-point approach, with one source typically a free-space blackbody target and the second a clear view to the cosmic microwave background, commonly referred to as "cold space." Occasionally, one or both of these calibration sources can become corrupted, either by solar/lunar intrusion in the cold space view or by thermal instability of the blackbody calibration source. A Temporal Experiment for Storms and Tropical Systems (TEMPEST) microwave sounder instrument is currently deployed on the International Space Station (ISS) for a 3-yr mission. TEMPEST is also calibrated using a blackbody target and cold space view; however, the cold space view will be routinely obstructed by objects present on the ISS. Here we test an alternative single-point calibration methodology that uses only the blackbody calibration target. We find the brightness temperature difference between this new approach and the traditional two-point calibration approach to be <0.1 K when applied to 3 years of the TEMPEST CubeSat Demonstration (TEMPEST-D) mission data from 2018 to 2020. This approach is applicable to other microwave radiometers that experience occasional degradation of calibration sources, such as thermal effects, intrusions, or instability of noise diodes.

SIGNIFICANCE STATEMENT: Cross-track microwave sounders have relied on two distinct calibration sources, often the cosmic microwave background using a clear view to cold space and an ambient blackbody target. We have tested an alternative approach that uses a single calibration target, making the sensor robust to occasional field-of-view intrusions of the space view or alternatively simplifies the spaceborne sensor design by eliminating the need for a clear view to space. We find that the performance difference between this new approach and the traditional two-calibration source approach is indistinguishable for both microwave temperature/water vapor profiling and precipitation-rate estimation. This calibration technique can be applied to past, current, and future microwave sounders to help diagnose systematic uncertainties in sensor calibration targets.

KEYWORDS: Microwave observations; Satellite observations; Soundings

1. Introduction

Passive microwave temperature and water vapor sounding instruments have been providing information on the atmospheric state from space on a global basis for over 40 years and are now critical for accurate forecasts from numerical weather prediction models (Bormann et al. 2013; Doherty et al. 2015; Li et al. 2016). The global operational record began with the Microwave Sounding Unit (MSU) and continued with the Advanced Microwave Sounding Unit (AMSU) and Advanced Technology Microwave Sounder (ATMS) (Homan and Soltis 1977; Aumann et al. 2003; Kim et al. 2014). While the technology has evolved over time, the basic calibration approach has remained the same. Spaceborne microwave radiometers are typically calibrated to determine antenna brightness from the measured voltage (or counts) using frequent observations of two points that bound the range of Earth-viewing brightness temperatures. Most often they comprise an ambient temperature free-space blackbody absorber and the cosmic microwave background using a clear view to cold space. Radiometers are generally designed to be linear systems, so only two points are needed to characterize the receiver gain (slope) and receiver noise temperature (offset). However, there are certain instances when one or the other target becomes corrupted, such as direct solar illumination of the blackbody load or lunar/solar intrusion in the cold space view (Kunkee et al. 2008). In these cases, the calibration is typically degraded for a period of an orbit. Methods to correct for or interpolate across these degraded periods have been developed with some success (Kigawa and Mo 2002; Mo and Kigawa 2007; Hu and Weng 2015). However, an alternative, computationally straightforward calibration approach capable of producing the same quality of calibration as the two-point approach would be desired.

In this study, we investigate a single-point calibration approach using on-orbit data from the Temporal Experiment for Storms and Tropical Systems Demonstration (TEMPEST-D) CubeSat microwave radiometer/sounder (Reising et al. 2018; Padmanabhan et al. 2021). This approach has been applied to the L-band Microwave Imaging Radiometer using Aperture Synthesis (MIRAS) radiometer on the *Soil Moisture Ocean Salinity* (*SMOS*) satellite, demonstrating that it is equivalent to or better than the two-point calibration approach for that receiver (Corbella et al. 2020). However, it has yet to be applied

Denotes content that is immediately available upon publication as open access.

Corresponding author: Shannon Brown, shannon.t.brown@jpl.nasa.gov

DOI: 10.1175/JTECH-D-22-0063.1

to microwave sounders operating at higher microwave frequencies up to 183 GHz. This study compares the calibration quality between the single-point and two-point calibration methods as applied to the TEMPEST-D sensor operating from 87 to 181 GHz. This study is motivated by the Space Test Program Houston-8 (STP-H8) mission which has deployed the TEMPEST flight spare unit on the International Space Station (ISS). TEMPEST-H8 uses the same blackbody target/cold space calibration approach as prior sounders; however, the cold space view is expected to be blocked by visiting spacecraft for periods of 3 or more months as well as at certain points in each orbit by the ISS solar arrays. During this time, only the warm blackbody target is available for calibration, and an alternative single-point calibration approach is required.

2. TEMPEST instrument description

The TEMPEST mission was originally conceived to provide greatly improved temporal resolution of global observations from LEO of convective precipitation over the ocean and the surrounding water vapor profile. The TEMPEST-D CubeSat demonstration satellite was designed, built, and deployed from the ISS in July 2018. It operated continuously on-orbit until it reentered Earth's atmosphere on 21 June 2021. TEMPEST-D is a 6U CubeSat carrying a cross-track-imaging, five-channel passive microwave radiometer with bands from 87 to 181 GHz. Critical to the TEMPEST design is the ability to accurately resolve the time derivative of the scene brightness temperature. This is facilitated by the inclusion of high-quality, blackbody calibration sources viewed through the antenna, end to end (Padmanabhan et al. 2021). In this way, the sensor design and data quality are similar to the ATMS on the NOAA LEO polar-orbiting operational satellites (Kim et al. 2014). A comprehensive intercalibration study using the double-difference method demonstrated that the TEMPEST-D calibration is statistically identical to the Global Precipitation Mission Microwave Imager (GMI) and the Microwave Humidity Sounder (MHS) sensors on ESA/EUMETSAT MetOp series satellites (Berg et al. 2021).

The TEMPEST-D CubeSat instrument, illustrated in Fig. 1, comprises a scanning antenna assembly, a single multifrequency feed horn, and five direct-detection microwave receivers. The five center frequencies are 87, 164, 174, 178, and 181 GHz. The antenna scans at 30 RPM in the cross-track direction, providing views of the Earth scene and two calibration targets. A blackbody absorber is viewed at the top of the scan in the zenith direction, and cold space is viewed approximately 90° from nadir. The blackbody absorber temperature is continuously monitored by thermistors mounted on the aluminum backplane. The radiometer integrates samples for 5 ms. The receivers use indium phosphide HEMT low-noise amplifiers, reducing the receiver noise temperature compared to other spaceborne radiometers at similar frequencies. The sensor mass is 3.8 kg, and it operates using only 6.5 W of power. The spatial resolution at nadir is 25 km for the 87-GHz channel and 12.5 km for the 164–181-GHz channels. The swath width is 1400 km.

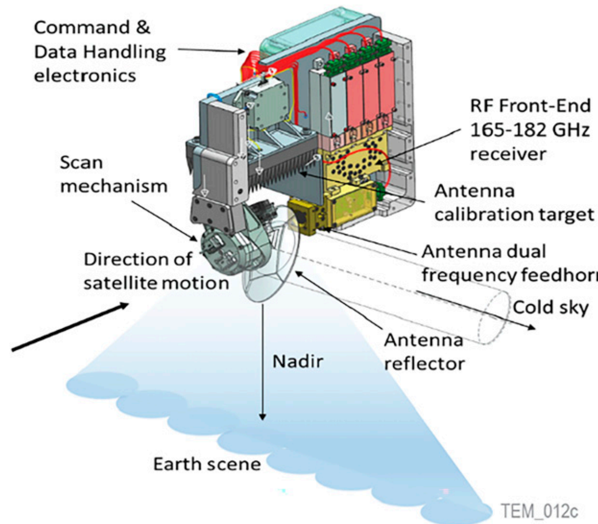

FIG. 1. CAD model of the TEMPEST-D CubeSat instrument. A single parabolic reflector rotates to scan the sensor across track. An ambient blackbody calibration target, internal to the instrument, is viewed in the zenith direction, and a clear view to cold space is viewed approximately 90° from nadir.

3. Single-point calibration

a. Motivation

Microwave radiometers are typically calibrated using at least two well-characterized sources to determine the receiver gain (slope) and noise temperature (offset). However, if one of these parameters is already known, then only a single point is needed. A single-point calibration technique was suggested and applied to the MIRAS radiometer (Corbella et al. 2020). In this study, the technique is applied to the TEMPEST-D microwave radiometer over its 3-yr mission. The original motivation for this study is the TEMPEST-H8 microwave radiometer.

TEMPEST-H8 was launched to the ISS on 21 December 2021 for a 3-yr Space Force technology demonstration mission. It was installed and powered up on 7 January 2022. TEMPEST-H8 was built as a flight spare to TEMPEST-D and is nearly identical, with only minor differences in radiometer passband response due to fabrication tolerances. TEMPEST-H8 is calibrated in the same manner as TEMPEST-D, using a free-space blackbody target and view to cold space. However, on the ISS, the cold space view can be blocked by docked spacecraft for several months at a time. Additionally, the ISS solar arrays rotate during an orbit and partially obstruct the cold space view for periods of an orbit. During these times, only the blackbody target is available for calibration, and a single-point calibration approach must be implemented. This study compares one-point calibration to two-point calibration using TEMPEST-D data, to quantify the expected sensor error during times of cold space blockage.

b. Single-point calibration technique

The radiometer antenna temperature can be calibrated from a single source using Eq. (1):

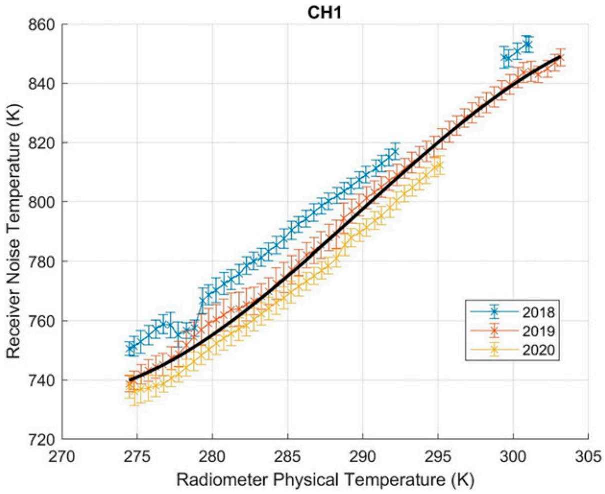

FIG. 2. TEMPEST-D 181-GHz receiver noise temperature averaged as a function of LNA temperature individually for the years 2018–20. The black line shows Eq. (2) fit to all data.

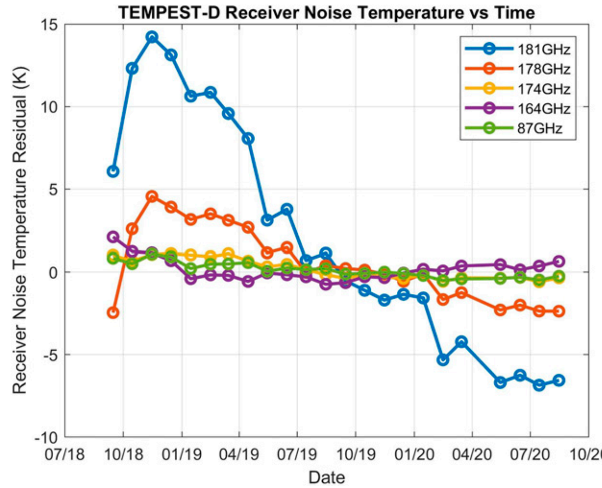

FIG. 3. Time variability of the TEMPEST-D receiver noise temperature averaged monthly after removal of the LNA temperature dependence from September 2018 to September 2020.

$$T_A = \left(\frac{v_A}{v_{\rm cal}} - 1\right)T_{\rm rec} + \frac{v_A}{v_{\rm cal}}T_{\rm cal}, \qquad (1)$$

where T_A is the calibrated antenna temperature, v_A and $v_{\rm cal}$ are the measured radiometer detector voltages looking at the scene of interest and at the calibration source, respectively, $T_{\rm rec}$ is the receiver noise temperature, and $T_{\rm cal}$ is the apparent brightness temperature of the calibration source (Corbella et al. 2020). In Eq. (1), both the receiver noise temperature and calibration source temperature must be known. Additionally, Eq. (1) assumes the receiver gain is linear. The calibration source in Eq. (1) could be a free-space blackbody target, cold space view, internal matched load, or noise diode, depending on the radiometer design. The calibration source temperature is assumed to be known with minimal uncertainty. The receiver noise temperature must be characterized in the laboratory before launch or in flight and typically varies with the physical temperature of the receiver and may drift with time. Therefore, the accuracy of the single-point calibration technique depends on how well the receiver noise temperature can be parameterized.

c. Receiver noise temperature parameterization

The receiver noise temperature is typically well characterized as a polynomial function of the receiver physical temperature, as shown in Eq. (2). The relevant component to track in the radiometer receiver is the temperature near the first low-noise amplifier (LNA) which determines the overall receiver noise temperature of the radiometer chain (assuming the radiometer follows basic design principles where the first LNA has sufficient gain to overcome the noise from the subsequent amplifiers in the chain). This temperature is measured with an uncertainty less than 0.05 K using a single thermistor on the metallic LNA housing that has a direct conductive path to the LNA chip. The LNA physical temperature is referenced to a nominal 300 K in Eq. (2), so that the a_0 term more meaningfully corresponds to the receiver noise temperature near room temperature (where prelaunch laboratory measurements are made). A third-order polynomial best fits the temperature dependence of the receiver noise temperature for TEMPEST-D. In general, the polynomial order must be empirically derived and depends on the amplifier used. Other radiometers may need higher- or lower-order polynomials to parameterize the receiver noise temperature. The temperature-dependent coefficients are assumed to be time invariant, though this is not a strict requirement. The offset term (a_0) is assumed to have some time variability that is unknown a priori and needs to be characterized. In practice, this can be accomplished by periodic two-point calibration during sensor operation (e.g., maneuvering the spacecraft to view cold space through the normal Earth-viewing portion of the scan) or by vicarious methods (e.g., using simulated brightness temperatures from weather model fields). The success and utility of the single-point calibration technique largely depends on having a minimal number of coefficients that must be characterized with time:

$$T_{\rm rec} = a_0(t) + \sum_{i=1}^{3} a_i(T_{\rm LNA} - 300)^i. \qquad (2)$$

4. Application to TEMPEST-D

a. TEMPEST-D receiver noise temperature characterization

The TEMPEST-D receiver noise temperature is computed once per scan (approximately every 2 s) as the antenna slews past the warm load (WL) blackbody target and the cold space (CS) view using

$$T_{\rm rec} = \frac{v_{\rm WL}(T_{\rm WL} - T_{\rm CS})}{v_{\rm WL} - v_{\rm CS}} - T_{\rm WL}, \qquad (3)$$

where $v_{\rm WL}$ and $v_{\rm CS}$ are the measured radiometer detector voltages when viewing the warm load and cold space view, respectively, and $T_{\rm WL}$ and $T_{\rm CS}$ are the brightness temperatures

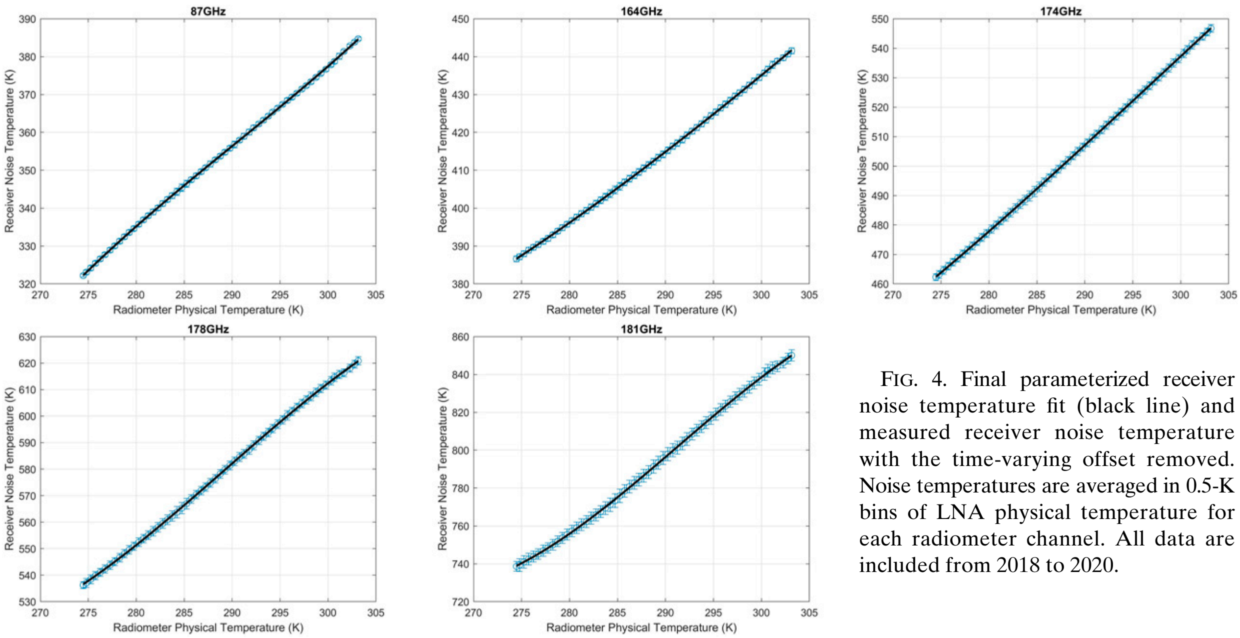

FIG. 4. Final parameterized receiver noise temperature fit (black line) and measured receiver noise temperature with the time-varying offset removed. Noise temperatures are averaged in 0.5-K bins of LNA physical temperature for each radiometer channel. All data are included from 2018 to 2020.

of each target. The TEMPEST-D LNA physical temperature varies from 274 to about 305 K over a year as the angle between the sun and the orbit plane varies (beta angle). The parameters in Eq. (2) are found by least squares fit of the computed receiver noise temperatures using Eq. (3) as a function of the LNA physical temperature. An example of the TEMPEST-D 181-GHz receiver noise temperature averaged in 1° bins of LNA physical temperature individually for the years 2018, 2019, and 2020 is shown in Fig. 2. The black line shows Eq. (2) fit to all data. This figure supports the assumption that the temperature-dependent terms may be held constant with time, which is verified by the subsequent analysis.

A two-step process is used to determine the final set of a_i coefficients. A first set of coefficients is fit by least squares regression to all the data over the 2018–20 time period using a single time-independent value for a_0. Next, the measured receiver noise temperatures are differenced from this initial parameterization to remove the temperature dependence leaving a time-dependent residual. A monthly average of this residual is shown in Fig. 3. The trends in Fig. 3 nominally represent the time-dependent component of the $a_0(t)$ term, a temporal drift in the receiver noise temperature. This drift is not unexpected for a component aging. For TEMPEST-D, it was found that time dependence could be adequately characterized by monthly averages. Other sensors may require higher- or lower-order parameterizations for the time dependence based on the amplifier behavior. For TEMPEST-D, the $a_0(t)$ term is represented by a lookup table comprising the monthly average values shown in Fig. 3. Linear interpolation is used for times between the monthly values. A second fit is performed to fine tune the a_i terms. The time-dependent biases from Fig. 3 [$a_0(t)$] are subtracted from the measured receiver noise temperatures to which the a_i terms are fit. The differences between the first and second fit were minor, as shown in Fig. 4.

Figure 3 shows that the receiver noise temperatures are remarkably stable in time. The 87 and 164 GHz channels are stable to approximately 1 K over the 3-yr dataset ($<$0.3%). The largest variation of about 22 K is observed in the 181-GHz channel ($<$3% of T_{rec}). The InP HEMT LNAs used in TEMPEST-D have an upper design limitation near 183 GHz and the gain begins to decrease over the 181-GHz channel bandwidth, which may explain this observation.

The error bars in Fig. 4 represent the standard deviation of all measured receiver noise temperature per 0.5-K bin of LNA temperature after removal of the time-dependent offset in Fig. 3. The residual difference between the parameterized

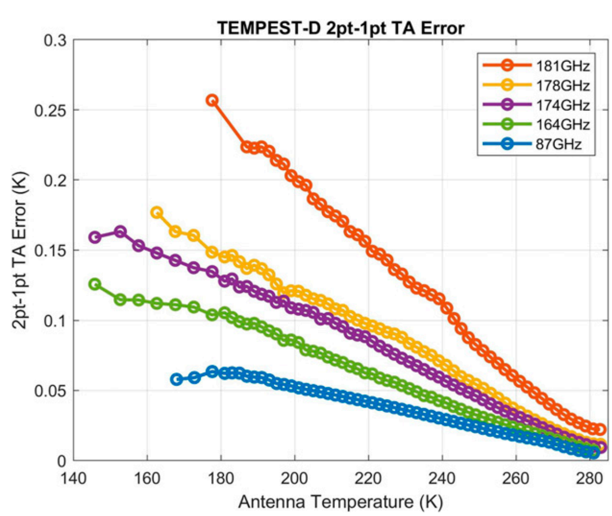

FIG. 5. Error between the single-point and two-point calibrated antenna temperature as a function of antenna temperature using TEMPEST-D data.

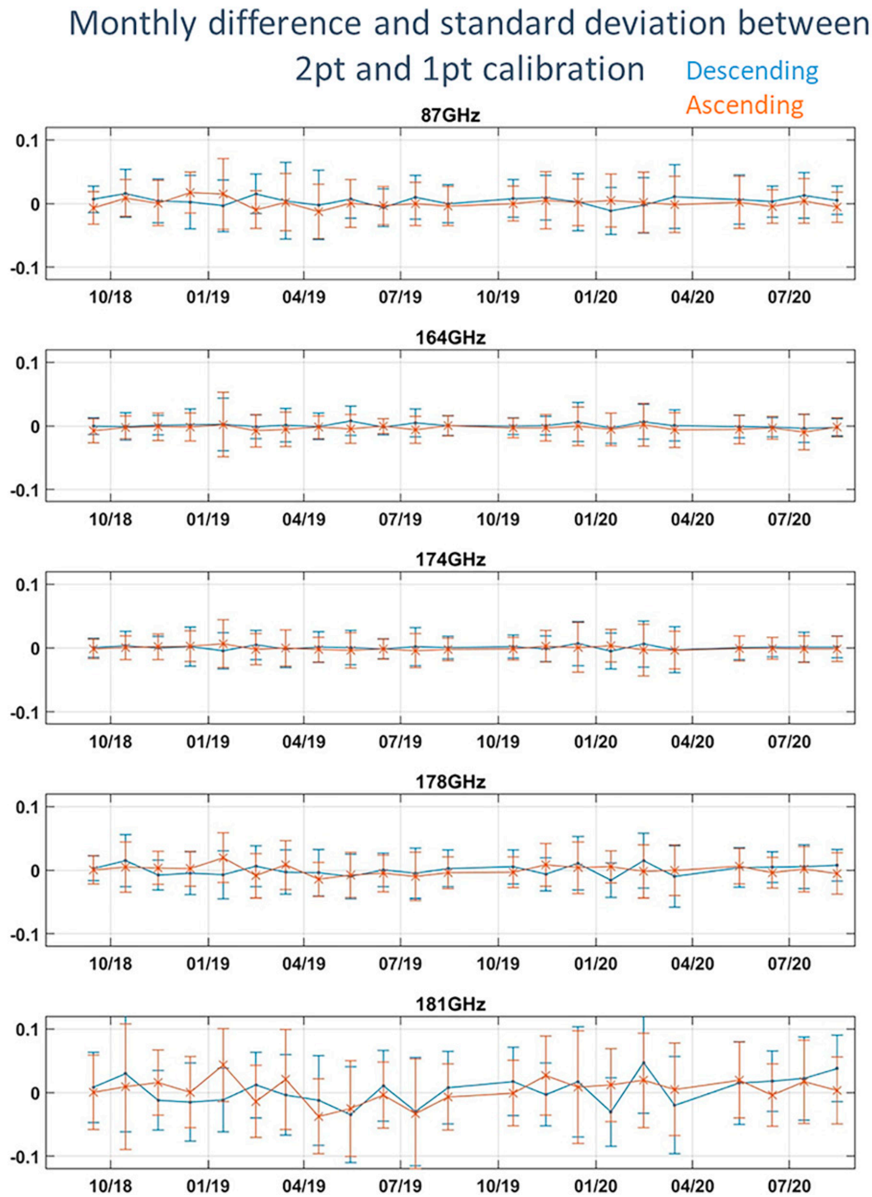

FIG. 6. Monthly mean and standard deviation of the difference between the single-point and two-point calibrated T_A values for each TEMPEST-D channel from September 2018 through September 2020. The blue line shows the descending passes, and the orange line shows the ascending passes.

T_{rec} using monthly updated offsets and the once per scan measured T_{rec} is 0.5, 0.5, 1.0, 1.2, and 2.3 K for the 87-, 164-, 174-, 178-, and 181-GHz channels, respectively. The white noise component of the measured T_{rec} has been removed when computing these values.

b. Comparison of single-point and two-point calibration

A prior study demonstrated that the performance and stability of the TEMPEST-D brightness temperatures (TBs) calibrated using the two-point method were statistically indistinguishable from the GMI and the MHS sensors (Berg et al. 2021). Therefore, the stability of the single-point calibration can intercompared with the nominal two-point calibrated TBs to quantify its performance. It can be shown that the error in the antenna temperature computed from Eq. (1) is related to uncertainty in the receiver noise temperature parameterization as (Corbella et al. 2020)

$$E(T_A) = \left(\frac{T_A + T_{\mathrm{rec}}}{T_{\mathrm{cal}} + T_{\mathrm{rec}}} - 1\right)\Delta T_{\mathrm{rec}}. \tag{4}$$

The error in T_A approaches zero as the calibration target temperature approaches the antenna temperature. For a microwave

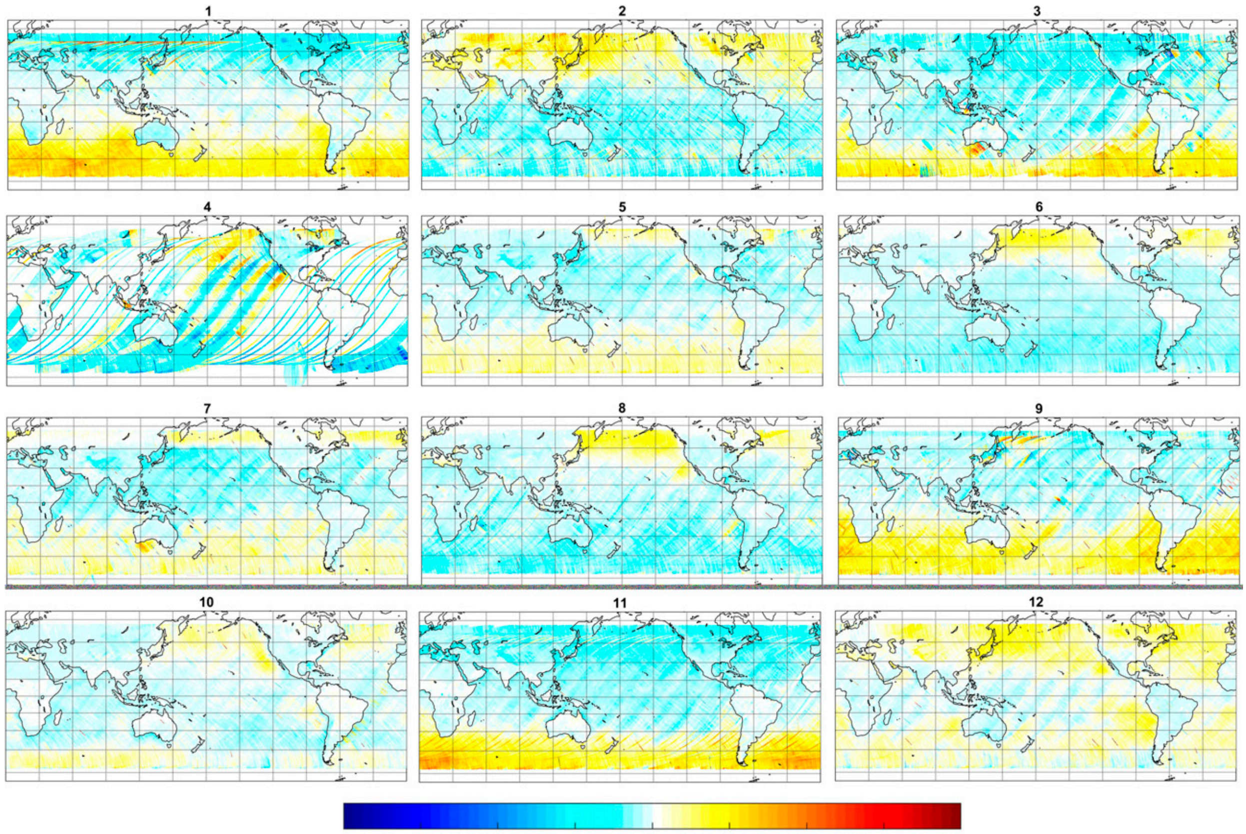

FIG. 7. Monthly average maps of the difference between single-point and two-point calibrated T_A values for the TEMPEST-D 87-GHz channel for ascending passes from September 2018 to September 2020.

sounder, it is advantageous to use the warm load blackbody target as the single calibration source, since this is typically much closer to the observed antenna temperature, which is generally above 200 K. Exceptions are observations of strong convection where ice scattering can depress the antenna temperature as low as 100–150 K. Using the residual errors of the parameterized $T_{\rm rec}$ in Eq. (4) and the mean receiver noise temperature from Fig. 4, the antenna temperature calibration error for a 200 K scene is 0.07, 0.06, 0.1, 0.1, and 0.2 K for the 87-, 164-, 174-, 178-, and 181-GHz channels, respectively. The error is less than half of those values for a T_A of 250 K. These errors are less than the receiver temperature noise floor for most radiometers.

To perform a direct comparison, TEMPEST-D data are calibrated using the nominal two-point method and the single-point method for 2018–20. Figure 5 shows the root-mean-square error between the two-point and single-point method as a function of antenna temperature for each channel. The slope of the error with antenna temperature is consistent with that predicted from Eq. (4) using the residual $T_{\rm rec}$ errors given above. Figure 6 shows the mean difference and standard deviation between single-point and two-point calibration for each 5-ms sample and for each month of the mission (all antenna temperatures). It should be noted that the radiometric resolution of the antenna temperature (NEDT) is common to both the single-point and two-point calibrated T_A in this comparison, so the standard deviation represents only the difference between the two calibration methods. The data are divided into ascending and descending passes. It is remarkable that the residual difference within a month is typically less than 0.05 K (1σ) for the 87–178-GHz channels and is less than 0.1 K (1σ) at 181 GHz. These results are consistent with the observed performance of the single-point calibration technique applied to the 1.4-GHz MIRAS radiometer (Corbella et al. 2020).

Monthly maps of the residual between the single-point and two-point calibration for the 87- and 164-GHz channels are shown in Figs. 7 and 8, respectively. The residuals are generally in the range of 0.05 K and have a clear geographic dependence. This dependence is not correlated with the LNA temperature. The systematic nature of this dependence suggests that there are small, but detectable errors in the knowledge of the TEMPEST-D calibration targets. A probable explanation is subtle variations in three-dimensional thermal gradients of the TEMPEST-D blackbody calibration target not tracked by the thermistors on the backside as the environmental forcing changes during the year (e.g., solar illumination angle, Earth infrared flux). A detailed explanation for these residuals is beyond the scope of this paper; however, it suggests that the single-point calibration method can be applied to other spaceborne microwave

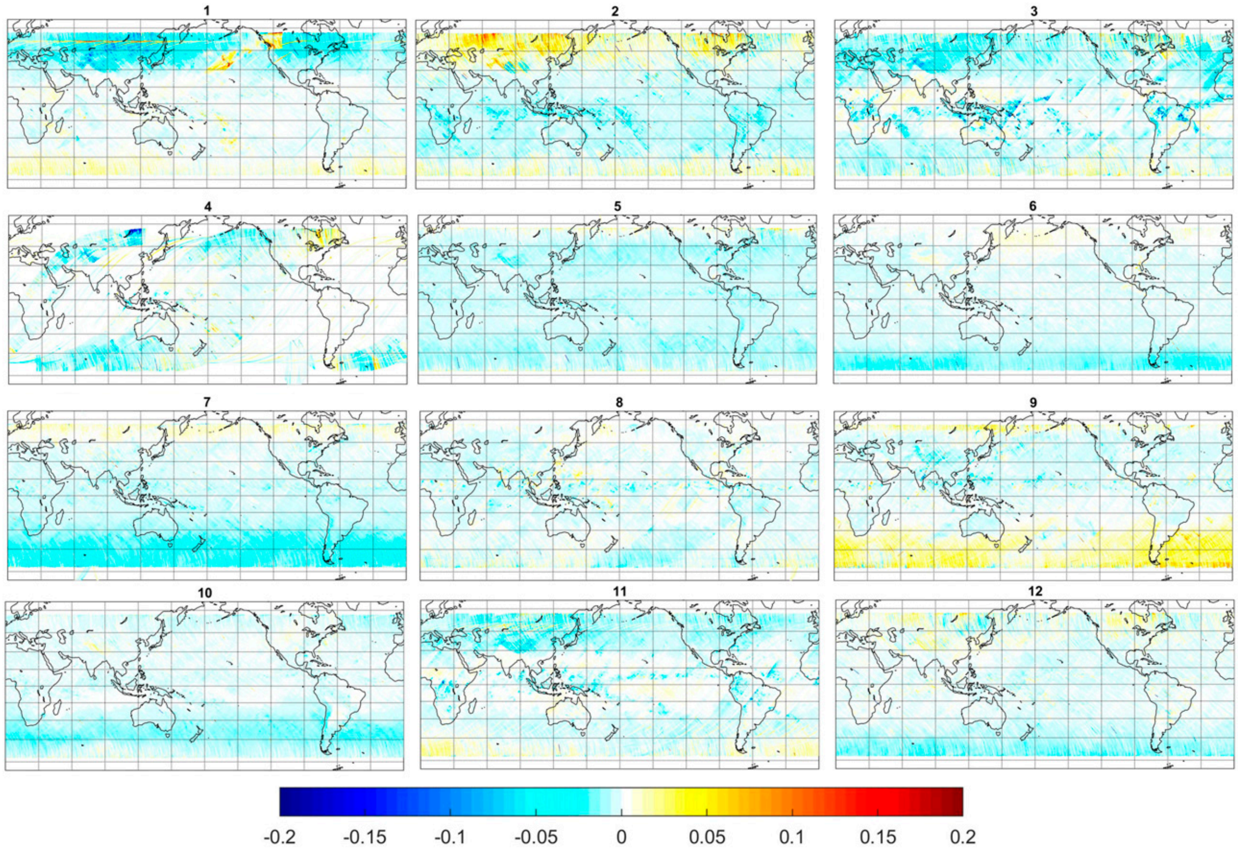

FIG. 8. Monthly average maps of the difference between single-point and two-point calibrated T_A values for the TEMPEST-D 164-GHz channel for ascending passes from September 2018 to September 2020.

radiometers to better characterize the quality of the onboard calibration sources.

5. Outlook for TEMPEST-H8

This study has demonstrated that the difference in TB computed using a single-point and two-point calibration approach is between 0.05 and 0.1 K (1σ) over the 3 years of the TEMPEST-D mission in low Earth orbit, with monthly updates to the receiver noise temperature. For TEMPEST-H8 on the ISS, the cold space view is expected to be blocked for periods of up to 3 months. The impact on calibration accuracy is conservatively assessed for a field-of-view blockage of up to 6 months. We estimate the worst-case residual receiver noise temperature temporal variation over any 6-month period from Fig. 3. The values range from less than 1 K at 90, 164, and 174 GHz to less than 7 K at 181 GHz. Using a calibration target temperature of 290 K, the error is estimated for sounding and for precipitation measurement using Eq. (4). A typical TB for atmospheric sounding is 250 K and a typical value for deep convective precipitation is 150 K. We note that the 181-GHz channel will rarely see TBs as low as 150 K, making this a conservative assessment for the channels closer to line center. The resulting errors are shown in Table 1. For a 250-K TB, the errors are in the range of 0.05–0.25 K. For a 150-K TB, which would be observed in deep convection, the error ranges from 0.2 to 0.9 K. These errors are nearly within the range of the single sample NEDT, and radiative transfer uncertainty for the two applications and would not appreciably degrade the respective retrievals. The errors would be about half of those listed in Table 1 for the anticipated 3-month blockage. It is noted that this analysis assumes TEMPEST-H8 will have similar T_{rec} stability as TEMPEST-D did.

6. Discussion and conclusions

This study has shown that a single-point calibration approach is a viable method for calibrating a microwave sounder

TABLE 1. Estimated error (K) for TEMPEST-H8, based on TEMPEST-D data, for a 6-month cold space field-of-view blockage for T_A = 150 and T_A = 250 K.

Channel	Max observed T_{rec} variation over 6 months	Max error at T_A = 150 K (Precipitation)	Max error at T_A =250 K (Sounding)
87 GHz	<1	<0.2	<0.06
164 GHz	<1	<0.2	<0.06
174 GHz	<1	<0.2	<0.05
178 GHz	<3	<0.5	<0.14
181 GHz	<7	<0.9	<0.25

using direct-detection receivers with 35-nm InP LNA front ends. The results from the TEMPEST-D CubeSat mission suggest that the method is equivalent to the two-point calibration approach when the receiver noise temperature is updated at least monthly. While the traditional two-point calibration approach will typically be superior to the single-point approach and is recommended for those sensors relied upon operationally for weather prediction and climate studies, there are cases where the single-point approach is beneficial. For example, future compact sensor designs (i.e., those on CubeSats or SmallSats) may consider a single calibration source if inclusion of two sources is impractical. In this case, a blackbody absorber source would be closer to the measured antenna temperatures, making it preferable to using cold space as the single calibration source. In practice, the receiver noise temperature time dependence (a_0) can be tracked by periodic two-point calibration by spacecraft maneuver to point to cold space or by using vicarious methods, such as comparison to a radiative transfer model. Several cold sky calibrations could be performed at different instrument temperatures to verify the temperature dependence. This could be performed by taking advantage of environmentally induced in-orbit thermal variations or by changing radiometer temperature set points if active thermal control is available, with the former method preferable since it best preserves the correlation between the thermistor measurement and amplifier temperature. This method can be used as an alternative to correction or interpolation techniques for two-point calibration sensors for periods when one of the calibration sources is degraded, due to solar/lunar intrusion or degraded thermal stability, a situation common even with operational sensors (Kigawa and Mo 2002; Mo and Kigawa 2007; Hu and Weng 2015). This method is also a useful diagnostic tool for assessing the quality of the sensor calibration targets. The residual difference between the two calibration methods applied to TEMPEST-D show a clear systematic geographic dependence. This suggests that the approach may be used to investigate or characterize uncertainties in the knowledge of on-orbit calibration target temperatures. Here also is an area where this methodology may benefit operational sensors, since characterizing systematic calibration errors is critical to accurate use in numerical weather prediction. It is noted that these results are particular to the InP HEMT front-end LNAs flown in TEMPEST-D. Future studies that perform this analysis with other spaceborne microwave radiometers, such as SSMIS, AMSU, and ATMS, would provide additional insight.

Acknowledgments. The research was carried out at the Jet Propulsion Laboratory, California Institute of Technology, under a contract with the National Aeronautics and Space Administration (80NM0018D0004) and at Colorado State University.

Data availability statement. All data used in this paper are publicly available after user registration at https://tempest.colostate.edu/data.

REFERENCES

Aumann, H. H., and Coauthors, 2003: AIRS/AMSU/HSB on the Aqua mission: Design, science objectives, data products, and processing systems. *IEEE Trans. Geosci. Remote Sens.*, **41**, 253–264, https://doi.org/10.1109/TGRS.2002.808356.

Berg, W., S. T. Brown, B. H. Lim, S. C. Reising, Y. Goncharenko, C. D. Kummerow, T. C. Gaier, and S. Padmanabhan, 2021: Calibration and validation of the TEMPEST-D CubeSat radiometer. *IEEE Trans. Geosci. Remote Sens.*, **59**, 4904–4914, https://doi.org/10.1109/TGRS.2020.3018999.

Bormann, N., A. Fouilloux, and W. Bell, 2013: Evaluation and assimilation of ATMS data in the ECMWF system. *J. Geophys. Res. Atmos.*, **118**, 12 970–12 980, https://doi.org/10.1002/2013JD020325.

Corbella, I., F. Torres, J. Closa, N. Duffo, I. Durán, V. González-Gambau, and M. Martín-Neira, 2020: One-point microwave radiometer calibration. *IEEE Geosci. Remote Sens. Lett.*, **17**, 461–463, https://doi.org/10.1109/LGRS.2019.2923539.

Doherty, A., N. Atkinson, W. Bell, and A. Smith, 2015: An assessment of data from the advanced technology microwave sounder at the Met Office. *Adv. Meteor.*, **2015**, 956920, https://doi.org/10.1155/2015/956920.

Homan, H. G., and F. Soltis, 1977: TIROS-N Microwave Sounder Unit (MSU)—Detail specification. JPL SPEC ES5 A 11746.

Hu, Y., and F. Weng, 2015: Corrections for on-orbit ATMS lunar contamination. *IEEE Trans. Geosci. Remote Sens.*, **54**, 1918–1924, https://doi.org/10.1109/TGRS.2015.2490198.

Kigawa, S., and T. Mo, 2002: An algorithm for correction of lunar contamination in AMSU-A data. NOAA Tech. Rep. NESDIS 111, 37 pp., https://repository.library.noaa.gov/view/noaa/12824.

Kim, E., C.-H. J. Lyu, K. Anderson, R. V. Leslie, and W. J. Blackwell, 2014: S-NPP ATMS instrument prelaunch and on-orbit performance evaluation. *J. Geophys. Res. Atmos.*, **119**, 5653–5670, https://doi.org/10.1002/2013JD020483.

Kunkee, D. B., S. D. Swadley, G. A. Poe, Y. Hong, and M. F. Werner, 2008: Special Sensor Microwave Imager Sounder (SSMIS) radiometric calibration anomalies—Part I: Identification and characterization. *IEEE Trans. Geosci. Remote Sens.*, **46**, 1017–1033, https://doi.org/10.1109/TGRS.2008.917213.

Li, J., P. Wang, H. Han, J. Li, and J. Zheng, 2016: On the assimilation of satellite sounder data in cloudy skies in numerical weather prediction models. *J. Meteor. Res.*, **30**, 169–182, https://doi.org/10.1007/s13351-016-5114-2.

Mo, T., and S. Kigawa, 2007: A study of lunar contamination and on-orbit performance of the NOAA 18 Advanced Microwave Sounding Unit–A. *J. Geophys. Res.*, **112**, D20124, https://doi.org/10.1029/2007JD008765.

Padmanabhan, S., and Coauthors, 2021: TEMPEST-D radiometer: Instrument description and prelaunch calibration. *IEEE Trans. Geosci. Remote Sens.*, **59**, 10 213–10 226, https://doi.org/10.1109/TGRS.2020.3041455.

Reising, S. C., and Coauthors, 2018: An Earth venture in-space technology demonstration mission for temporal experiment for storms and tropical systems (TEMPEST). *2018 IEEE Int. Geoscience and Remote Sensing Symp.*, Valencia, Spain, Institute of Electrical and Electronics Engineers, 6301–6303, https://doi.org/10.1109/IGARSS.2018.8517330.